Fine structure of the isoscalar giant quadrupole resonance in ^{28}Si and ^{27}Al

I. T. Usman,[1,2,*] Z. Buthelezi,[2] J. Carter,[1] G. R. J. Cooper,[3] R. W. Fearick,[4] S. V. Förtsch,[2] H. Fujita,[1,2,5] Y. Fujita,[5] P. von Neumann-Cosel,[6,†] R. Neveling,[2] P. Papakonstantinou,[7] I. Pysmenetska,[6] A. Richter,[6] R. Roth,[6] E. Sideras-Haddad,[1] and F. D. Smit[2]

[1]*School of Physics, University of the Witwatersrand, Johannesburg 2050, South Africa*
[2]*iThemba LABS, P.O. Box 722, Somerset West 7129, South Africa*
[3]*School of Earth Sciences, University of the Witwatersrand, Johannesburg 2050, South Africa*
[4]*Department of Physics, University of Cape Town, Rondebosch 7700, South Africa*
[5]*Research Center for Nuclear Physics, Osaka University, Ibaraki, Osaka 567-0047, Japan*
[6]*Institut für Kernphysik, Technische Universität Darmstadt, D-64289 Darmstadt, Germany*
[7]*Rare Isotope Science Project, Institute for Basic Science, Daejeon 34047, Korea*

(Received 17 June 2016; published 5 August 2016)

The isoscalar giant quadrupole resonance in ^{28}Si and ^{27}Al has been investigated with high-energy-resolution proton inelastic scattering at $E_p = 200$ MeV and at scattering angles close to the maximum of $\Delta L = 2$ angular distributions with the K600 magnetic spectrometer of iThemba LABS, South Africa. Characteristic scales are extracted from the observed fine structure with a wavelet analysis and compared for ^{28}Si with random-phase approximation and second random phase approximation calculations with an interaction derived from the Argonne V18 potential by a unitary transformation. A recent extension of the method to deformed nuclei provides the best description of the data, suggesting the significance of Landau damping.

DOI: 10.1103/PhysRevC.94.024308

I. INTRODUCTION

High-energy-resolution inelastic proton scattering data obtained at beam energies of a few hundred MeV with magnetic spectrometers in combination with dispersion matching techniques provide a suitable approach to study the fine structure of the isoscalar giant quadrupole resonance (ISGQR) in nuclei. The necessary experimental techniques to perform (p,p') experiments with an energy resolution better than the energy spread of the incident projectile beam are discussed in Ref. [1] and for the experiments discussed here using the K600 spectrometer at iThemba LABS the relevant techniques are discussed in Ref. [2].

For a quantitative analysis of the observed fine structure, wavelet techniques have been shown to be most useful [3]. A systematic study of the ISGQR in medium- to heavy-mass nuclei [4,5] showed that scales characterizing the fine structure originate from a collective damping mechanism induced by the coupling of elementary one-particle one-hole (1p1h) states to low-lying surface vibrations [6]. In contrast, Landau damping (i.e., fragmentation on the 1p1h level) significantly contributes to the fine structure of the isovector giant dipole resonance [7]. Such conclusions were based on the comparison of random-phase approximation (RPA) calculations with more refined approaches allowing for a coupling of the 1p1h excitations to two-particle–two-hole (2p2h) states.

Recently, a high-energy-resolution measurement of the ISGQR in ^{40}Ca was performed [8], motivated by the question of whether collective damping remains the most important decay mechanism in lighter nuclei or if other mechanisms might play a leading role [9]. From a comparison of RPA and second-RPA (SRPA) calculations with a realistic interaction derived from the unitary correlation operator method (UCOM), it was concluded that Landau damping produces all but the lowest scale derived from the wavelet analysis [8]. The importance of Landau damping obtained with the UCOM interaction is in contrast to many RPA results for the ISGQR in ^{40}Ca with phenomenological interactions (see references in Ref. [8]) that all predict a single collective state and correspondingly no fine structure.

The present work extends these investigations to an even lighter nucleus, ^{28}Si. The fine-structure properties are compared with those of RPA and SRPA calculations in the framework discussed in Ref. [8]. Because ^{28}Si is an open-shell nucleus in the middle of the *sd* shell with a deformed ground state (g.s.), the SRPA approach was modified to define a g.s. wave function using shell-model occupation numbers for the valence orbits. Alternatively, a new approach based on a deformed Hartree-Fock g.s. [10] is tested. The impact of coupling a single particle (or hole) to an even-even core on the fine structure of the ISGQR is studied by an experimental comparison with the isotonic nucleus ^{27}Al. In the following, we discuss experiments, model calculations, and extractions of scales first and in greater detail for ^{28}Si and then for ^{27}Al.

II. EXPERIMENTAL RESULTS

A. Experiment and spectra

The experiments were carried out with a 200-MeV proton beam produced by the separated sector cyclotron (SSC) of the iThemba Laboratory for Accelerator Based Sciences (iThemba LABS), South Africa. The protons were scattered inelastically from self-supporting targets of ^{nat}Si (92.2% ^{28}Si) and ^{27}Al

*iyabo.usman@wits.ac.za
†vnc@ikp.tu-darmstadt.de

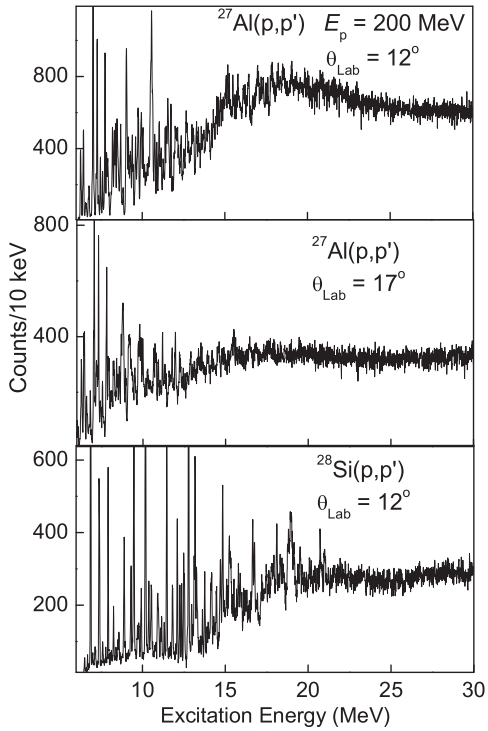

FIG. 1. Excitation energy spectra for ^{27}Al(p,p') reactions between 6 and 30 MeV at $E_p = 200$ MeV and $\theta_{\rm Lab} = 12^\circ$ (top panel) and $\theta_{\rm Lab} = 17^\circ$ (middle panel) and for the ^{28}Si(p,p') reaction at $\theta_{\rm Lab} = 12^\circ$ (bottom panel) covering low-lying states and the energy region of the ISGQR.

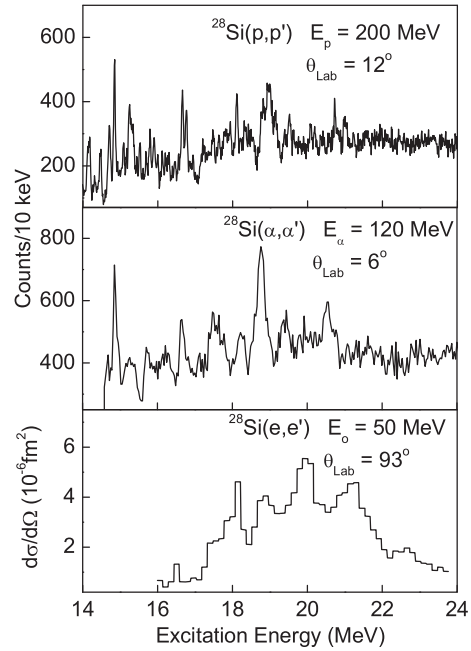

FIG. 2. Excitation energy spectra for the ISGQR in ^{28}Si from different probes: ^{28}Si(p,p') (present work), ^{28}Si(α,α') [12], and ^{28}Si(e,e') [13].

with areal densities of 0.232 and 0.819 mg/cm^2, respectively, and then momentum analyzed with the K600 magnetic spectrometer. Dispersion-matching techniques were used to exploit the high-energy-resolution capability of the spectrometer. A scattering angle of $\theta_{\rm Lab} = 12^\circ$ close to the maximum of the cross section for $\Delta L = 2$ transitions populating the ISGQR was selected. Details of the data analysis procedures are described in Ref. [11].

The excitation energy spectrum for the nucleus ^{28}Si is shown in the bottom panel of Fig. 1 for the full energy-bite of the K600 magnetic spectrometer, $6 \leqslant E_x \leqslant 30$ MeV. An energy resolution of $\Delta E = 38$ keV (full width at half maximum, FWHM) was achieved. A broad peak about 5 MeV wide between about 14 and 25 MeV centered at $E_{\rm x} \approx 18$ MeV resulting from excitation of the ISGQR can be identified. This is consistent with features of the ISGQR in ^{28}Si observed in (α,α') scattering [12]. Many discrete states below the respective proton (11.584 MeV) and neutron (17.178 MeV) thresholds in ^{28}Si are resolved, and above these thresholds, the fine structure is clearly visible in the energy region of the ISGQR. For ^{27}Al at the same scattering angle (upper panel of Fig. 1) a very similar behavior is found. In the middle panel of Fig. 1, a spectrum of ^{27}Al measured at $\theta_{\rm Lab} = 17^\circ$ is displayed. Here, the ISGQR bump is significantly reduced with respect to the background originating from other multipoles and quasifree reactions. However, in analogy to the case of ^{40}Ca a cross-correlation analysis [8] of the two spectra assures that the visible fine structure originates from the ISGQR.

B. Comparison of different probes exciting the ISGQR in ^{28}Si

For *sd*-shell nuclei with $A \leqslant 32$, extensive experimental investigations have been made on the fragmentation of the ISGQR. Results from proton (present work), α [12], and electron [13] scattering for the case of ^{28}Si are compared in Fig. 2.

Van der Borg *et al.* [12] investigated the properties of the ISGQR for a variety of *sd*-shell nuclei using (α,α') scattering at $E_\alpha = 120$ MeV with a resolution $\Delta E = 125$ keV (FWHM). The resulting ^{28}Si(α,α') excitation energy spectrum at $\theta_{\rm Lab} = 6^\circ$ is shown in the middle panel of Fig. 2. At this angle, many of the states excited in the energy range of 14–22 MeV were identified to have spin-parity $J^\pi = 2^+$ from angular distribution measurements, and excitation of the ISGQR was found to dominate over other isoscalar modes ($E0$, $E3$). There is good correspondence of the main structures except for an overall shift of the excitation energies of a few hundred keV.

The $E2$ strength distribution in ^{28}Si has also been measured with α scattering by the Texas A&M group and overall fair agreement has been found [14]. These data are not included in the further analysis because spectra for kinematics where $E2$ cross sections dominate were not available and the overall energy resolution was 250–300 keV (FWHM) only.

Additional comparison is made with ^{28}Si(e,e') data at low momentum transfers [13]. The lower panel in Fig. 2 displays the $B(E2)$ strength distribution extracted from a form factor

decomposition. The structures at 18–19 MeV and around 21 MeV agree with the peaks in the α and proton scattering data. An additional pronounced structure is visible around 20 MeV that is absent in the hadron scattering data. In contrast to the dominance of isoscalar excitations in proton and α scattering, electron scattering also excites isovector transitions, indicating isospin $T = 1$ for the structure at 20 MeV.

III. MODEL CALCULATIONS

Isoscalar $E2$ strength distributions were calculated using the RPA and the SRPA formalisms [15,16] with an effective interaction derived from the realistic Argonne V18 nucleon-nucleon interaction in the framework of the UCOM, as described in Ref. [17]. The same model was used in Ref. [8] to analyze the fine structure of the ISGQR in ^{40}Ca. A single-particle space of 13 harmonic-oscillator shells was used here to obtain the Hartree-Fock (HF) reference state and all HF single-particle states are included in the 1p1h and 2p2h spaces. The RPA and SRPA matrix elements are renormalized as described in Ref. [16] with occupation numbers taken from a $4\hbar\omega$ shell-model calculation. This hybrid model allows for the activation of sd states as particle and hole states to take into account the open-shell character of ^{28}Si. We further exclude low-energy 1p1h and 2p2h configurations within the sd shell to avoid unphysical solutions owing to the approximate description of the sd shell.

The above models do not explicitly take into account deformation. Therefore, theoretical $E2$ distributions were calculated also in the RPA using an axially deformed HF ground state and applying angular-momentum projection techniques [10]. Both the HF and the RPA calculations use the same realistic nucleon-nucleon interaction derived from the Argonne V18 potential by a unitary transformation in the framework of the (UCOM) and the similarity renormalization group as described in Refs. [18,19] and are supplemented by a phenomenological three-nucleon contact interaction. This Hamiltonian was introduced and tested in Ref. [20] for ground-state observables and applied to RPA calculations in closed-shell nuclei in Ref. [21] [we use the version labeled "S-UCOM(SRG)"]. All calculations were performed in a harmonic-oscillator single-particle basis covering 15 oscillator shells. Further details on the deformed RPA approach employed in this work can be found in Ref. [10].

The experimental spectra have a finite-energy resolution while the RPA and SRPA models provide a discretized strength distribution. Therefore, for the purposes of a direct comparison between experiment and theory independent of the resolution, the calculations were smoothed with a Gaussian function of width $\Delta E = 38$ keV (FWHM) and put into a bin size of 10 keV. Figure 3 summarizes the results of the RPA and SRPA predictions for ^{28}Si. It can be seen that the ISGQR is spread out widely. The differences between RPA and SRPA (middle and lower panels) results are small. The main effect is an overall shift of about 2 MeV lower in excitation in the SRPA calculation while the coupling to 2p2h states produces little additional fragmentation. The RPA calculation based on a deformed HF ground state (top panel of Fig. 3) finds a similar distribution in energy but shows significantly more structure.

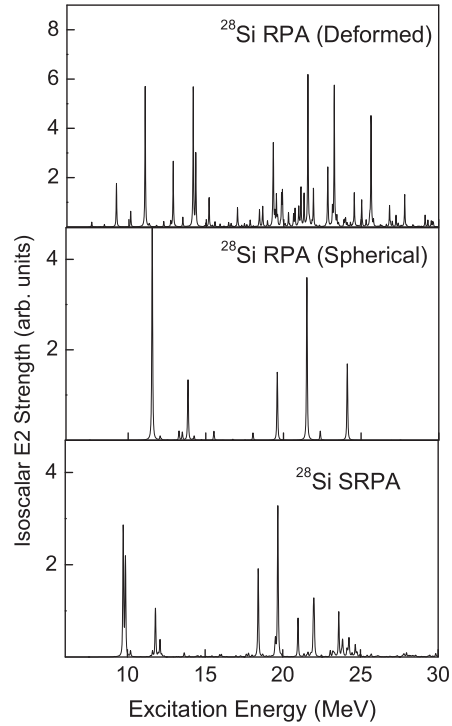

FIG. 3. RPA and SRPA isoscalar $E2$ strength distributions for ^{28}Si from the models described in the text. The discrete distributions are smoothed with the experimental energy resolution for direct comparison to the experimental data.

IV. EXTRACTION OF CHARACTERISTIC ENERGY SCALES

A. Wavelet analysis

The main aim of the present study is to extract characteristic energy scales within the excitation energy region of the ISGQR in the experimental data and compare those scales to the ones obtained from the corresponding theoretical strength functions. To quantitatively investigate the observed structures, wavelet analysis techniques [3,5,8] were utilized. A wavelet analysis of the data was accomplished using the MATLAB program [22].

A wavelet transform is defined as a convolution of the original energy spectrum $\sigma(E)$ multiplied by a scaled, shifted version of the wavelet function Ψ. The coefficients $(E_x,\delta E)$ of the wavelet transform are obtained as

$$C(E_x,\delta E) = \frac{1}{\sqrt{\delta E}} \int \sigma(E)\Psi\left(\frac{E_x - E}{\delta E}\right) dE, \qquad (1)$$

where δE is the scale and E_x is the position along the energy scale, respectively.

The parameters (excitation energy, E_x, and scale, δE) can be varied continuously (continuous wavelet transform, CWT) or in discrete steps j, where $\delta E = 2^j$, $j = 1, 2, 3, \ldots$, and $E_x = \delta E$. A variety of wavelets provide a set of tools for performing many different tasks. The choice of a particular wavelet is based on its mathematical properties [22,23], among which are moments, compact support, and the regularity of a signal (the number of times that it is continuously differentiable).

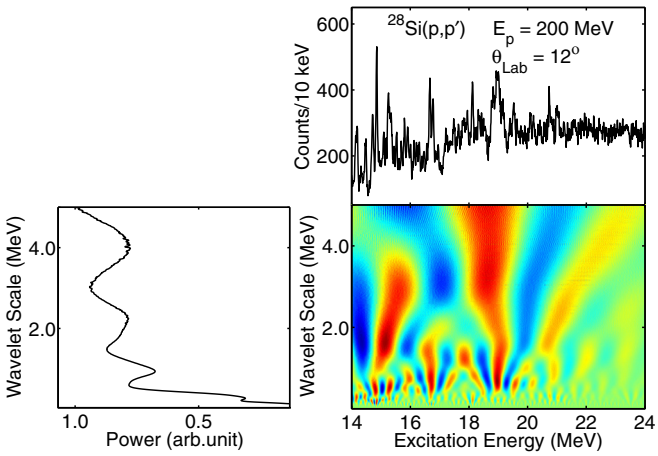

FIG. 4. Upper-right panel: Excitation energy spectrum of the ^{28}Si(p,p) reaction at a scattering angle of $\theta_{\rm Lab} = 12^\circ$ corresponding to the maximum cross section for excitation of the ISGQR. Lower-right panel: The CWT after applying a complex Morlet mother wavelet, red indicates large positive coefficients and blue large negative coefficients. Lower-left panel: Power spectrum in which the maxima of the peaks correspond to the values of characteristic energy scales.

Complex wavelets produce a complex wavelet transform, allowing the phase of the result to be examined. The choice of a mother wavelet is motivated by the type of spectrum being analyzed. The Morlet mother wavelet used in this analysis is derived by taking a periodic wave and localizing it with a Gaussian envelope:

$$\Psi(x) = \frac{1}{\pi^{1/4}} \exp(ikx) \exp\left(-\frac{x^2}{2}\right). \tag{2}$$

Here, the parameter k weighs the resolution in scales *versus* the resolution in localization. A value of $k = 5$ was chosen in the present work.

B. Application to ^{28}Si and ^{27}Al

A CWT was applied to the excitation energy region of the ISGQR in the spectra of Fig. 1 with a Complex Morlet mother wavelet. It should be emphasized, however, that before the application input data preparation is essential to minimize end effects. In our case, the mean of the input data set was subtracted from the data set before applying the wavelet technique. By plotting the real part of the complex coefficients on a two-dimensional plot of scale *versus* excitation energy, the positions of the structures within the original energy spectrum can be identified as illustrated in the lower-right panel of Fig. 4 for the ^{28}Si(p,p') experimental data. The maximum scale was restricted to 5 MeV to show the detail in substructures existing at smaller energy scales. To obtain the corresponding power spectrum, the square root of the sum of the squares of the complex coefficients are summed across onto the scale axis. The resulting power spectrum is shown in the lower-left panel of Fig. 4. It exhibits pronounced peaks representing characteristic energy scales of the structures in the spectrum.

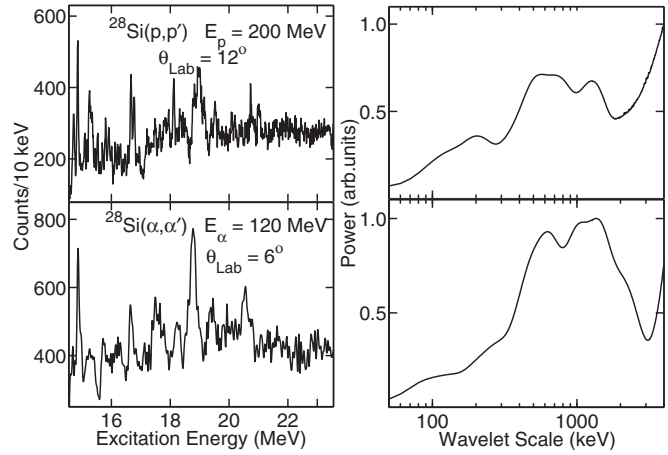

FIG. 5. Comparison of the CWT power spectra for the energy region of the ISGQR from the ^{28}Si(p,p') and (α,α') spectra.

It is instructive to compare the wavelet analysis results for the ISGQR in ^{28}Si from the (p,p') and (α,α') data sets (Fig. 5). The power spectra in the right-hand panels of Fig. 5 show very similar scales, i.e., maxima at a certain energy, as one would expect from the similarity of the spectra. The power maximum around 1 MeV exhibits comparable peaks but as a result of the better energy resolution the (p,p') data lead to more structure in the power spectrum at smaller scale values. The largest scales are affected by the shape of the physical background and the peak-to-background ratio leading to the observed differences in power values.

A summary of the power spectra from the CWT analysis for the present high-resolution (p,p') data in the energy region of the ISGQR in ^{28}Si and ^{27}Al and the corresponding theoretical isoscalar $E2$ strength distributions (see Fig. 3) is given in Fig. 6. The choice and suitability of wavelet functions for the analysis of nuclear giant resonances were

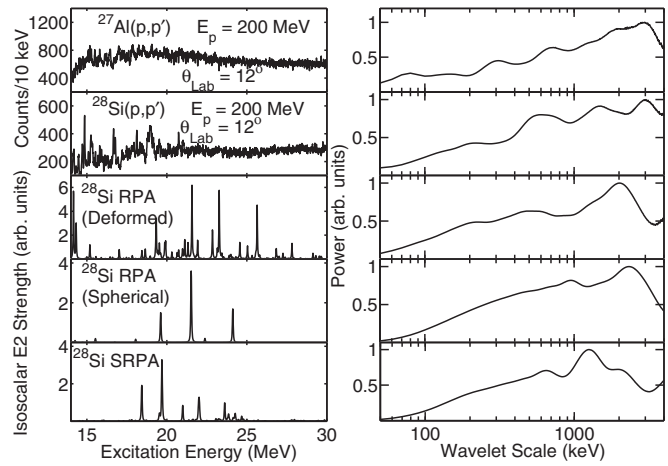

FIG. 6. Left-hand panels: Excitation energy spectra of ^{27}Al and ^{28}Si at the scattering angle of $\theta_{\rm Lab} = 12^\circ$ corresponding to the maximum cross sections for excitation of the ISGQR and theoretical strength distributions from RPA and SRPA. Right-hand panels: Corresponding power spectra from the CWT.

TABLE I. Summary of energy scales of the ISGQR in ^{27}Al and ^{28}Si and comparison with RPA and SRPA calculations for ^{28}Si.

			Class I <300 keV		Class II 300–1000 keV		Class III >1000 keV	
^{27}Al	Expt.	80	140		310	700	2000	2800
^{28}Si	Expt.		130	220		600	1500	3000
^{28}Si	RPA def.			250		500	1250	2000
^{28}Si	RPA sph.						1000	2400
^{28}Si	SRPA					650	1250	2000

discussed extensively in Ref. [3]. However, in the present analysis a Complex Morlet function was chosen since the resulting energy scales extracted are directly comparable to those obtained from a Fourier analysis. In previous analyses of the ISGQR in heavier nuclei [3,4] a real Morlet wavelet was used and the extracted scales need to be divided by a factor of 0.813 to yield the corresponding Fourier scale. Characteristic scales deduced from the power spectra are summarized in Table I. In passing we note that an earlier performed CWT analysis of the ^{28}Si(p,p') and (α,α') spectra (but without the above-mentioned input data preparation) gave results very similar to those in the present work [24]. Analogous to previous studies of scales of the ISGQR [4,5,8] the scales are grouped into three classes: <300 keV (Class I), 300–1000 keV (Class II), and >1000 keV (Class III).

One finds two broad (Class III) scales in the ^{28}Si data and in all calculations. However, a quantitative comparison is limited. In particular, the largest scale in the data is underestimated by all models. This may be related to the neglect of coupling to the continuum, which is known to make significant contributions to the resonance width in light nuclei. One intermediate (Class II) scale is observed in the data as well as in the RPA calculations on a deformed ground state. In contrast, the spherical RPA results show no Class II scales, but the SRPA predicts one scale in fair agreement with the experimental values. None of the three nuclear models is capable of reproducing both Class I scales in ^{28}Si, but the deformed RPA calculations account for the larger one, indicating that scales between 200 and 1000 keV result dominantly from Landau fragmentation.

Similar to the case of ^{40}Ca [8], no interpretation based on the model calculations can be given for the smallest scale in the data at 130 keV. Corresponding scales around 100 keV were found in all analyses of the ISGQR in heavier nuclei, but these could be clearly related to the coupling to low-energy phonons [4,5]. Here, the SRPA is performed in the diagonal approximation (i.e., the coupling among 2p2h states is ignored), leading to many near-degenerate eigenstates. Inclusion of the 2p2h-2p2h interaction pushes the spacing distribution towards the Wigner limit by level repulsion with a maximum average spacing at larger distances [25], which may produce a characteristic scale in the wavelet analysis. We have tested the idea with calculations in a limited energy range and model space for the case of ^{40}Ca and ^{28}Si and found it to be qualitatively consistent with our speculation.

Another possible interpretation of the lowest scale is that it originates from Ericson fluctuations [26], i.e., the scale represents the coherence width of overlapping 2^+ resonances. The coherence width in ^{28}Si has been discussed, e.g., in Ref. [27] and amounts to about 60 keV in the excitation region of the ISGQR. While the experiments quoted in Ref. [27] usually cover a larger spin window, the selectivity of the present data on $J^\pi = 2^+$ states leads one to expect a larger value for the coherence width that could well be of the order of the experimentally observed scale.

Finally, we briefly discuss a comparison of the scales in ^{28}Si with those in the odd-mass isotone ^{27}Al. All scales found in ^{28}Si appear in ^{27}Al as well. Typically, the values in the latter are slightly larger except for the broadest scale. Thus, the coupling of the unpaired proton seems to have little influence on the fine structure. However, an additional scale at 80 keV appears in ^{27}Al that may be interpreted to arise from the coupling of the unpaired proton (hole) to an even-even core. Therefore, we have observed that there is little influence of coupling a single particle (or hole) to an even-even core on the fine structure of the ISGQR, which has yet to be proven by theoretical calculations.

V. SUMMARY

The ISGQR excited in the nuclei ^{27}Al and ^{28}Si has been investigated using inelastic proton scattering at 200 MeV. Characteristic energy scales have been extracted by applying wavelet analysis techniques. To reveal the physical nature of observed scales, a comparison to results from RPA and SRPA calculations has been made for the case of ^{28}Si where the open-shell ground state has been approximated by shell-model occupation numbers for levels near the Fermi surface. Alternatively, RPA calculations were performed based on a deformed HF ground state. Clearly, the RPA calculations in a deformed basis provide a more realistic description of the experimentally observed fragmentation of the ISGQR. They qualitatively account for all but the smallest experimentally observed scale and indicate Landau fragmentation driven by deformation as the most important mechanism of the fine structure. As for ^{40}Ca, the smallest experimental scale at 130 keV in ^{28}Si cannot be explained by any of the models. It may be related to the neglect of coupling among the 2p2h states in the SRPA claculations or it may result from Ericson fluctations. A comparison of the ISGQR in the neighboring odd-mass isotone ^{27}Al reveals little difference except for an additional scale at 80 keV that may be interpreted to arise from the coupling of the unpaired proton.

ACKNOWLEDGMENTS

We are indebted to L. Conradie and the accelerator crew at iThemba LABS for providing excellent beams. This work has been supported by the South African NRF, the DFG under Contract No. SFB 1245, and the Rare Isotope Science Project of the Institute for Basic Science funded by the Ministry of Science, ICT and Future Planning, and the National Research Foundation of Korea (Grant No. 2013M7A1A1075764). I.T.U acknowledges the incentive funding for rated researcher support from the South African NRF.

[1] Y. Fujita, *et al.*, Nucl. Instrum. Methods Phys. Res., Sect. B **126**, 274 (1997).

[2] R. Neveling *et al.*, Nucl. Instrum. Methods Phys. Res., Sect. A **654**, 29 (2011).

[3] A. Shevchenko, J. Carter, G. R. J. Cooper, R. W. Fearick, Y. Kalmykov, P. von Neumann-Cosel, V. Yu. Ponomarev, A. Richter, I. Usman, and J. Wambach, Phys. Rev. C **77**, 024302 (2008).

[4] A. Shevchenko, J. Carter, R. W. Fearick, S. V. Förtsch, H. Fujita, Y. Fujita, Y. Kalmykov, D. Lacroix, J. J. Lawrie, P. von Neumann-Cosel, R. Neveling, V. Yu. Ponomarev, A. Richter, E. Sideras-Haddad, F. D. Smit, and J. Wambach, Phys. Rev. Lett. **93**, 122501 (2004).

[5] A. Shevchenko, O. Burda, J. Carter, G. R. J. Cooper, R. W. Fearick, S. V. Förtsch, H. Fujita, Y. Fujita, Y. Kalmykov, D. Lacroix, J. J. Lawrie, P. von Neumann-Cosel, R. Neveling, V. Yu. Ponomarev, A. Richter, E. Sideras-Haddad, F. D. Smit, and J. Wambach, Phys. Rev. C **79**, 044305 (2009).

[6] G. F. Bertsch, P. F. Bortignon, and R. A. Broglia, Rev. Mod. Phys. **55**, 287 (1983).

[7] I. Poltoratska, R. W. Fearick, A. M. Krumbholz, E. Litvinova, H. Matsubara, P. von Neumann-Cosel, V. Yu. Ponomarev, A. Richter, and A. Tamii, Phys. Rev. C **89**, 054322 (2014).

[8] I. Usman *et al.*, Phys. Lett. B **698**, 191 (2011).

[9] M. N. Harakeh and A. van der Woude, *Giant Resonances: Fundamental High-Frequency Modes of Nuclear Excitation* (Oxford University, Oxford, 2001).

[10] B. Erler and R. Roth, arXiv:1409.0826.

[11] I. T. Usman, PhD. thesis, University of the Witwatersrand, 2009.

[12] K. van der Borg, M. N. Harakeh, A. van der Woude, and F. E. Bertrand, Nucl. Phys. A **341**, 219 (1980).

[13] A. Friebel, Doctoral thesis D17, Technische Hochschule Darmstadt, 1981; A. Richter, Prog. Part. Nucl. Phys. **13**, 1 (1985).

[14] D. H. Youngblood, Y.-W. Lui, and H. L. Clark, Phys. Rev. C **76**, 027304 (2007).

[15] P. Papakonstantinou and R. Roth, Phys. Lett. B **671**, 356 (2009).

[16] P. Papakonstantinou and R. Roth, Phys. Rev C **81**, 024317 (2010).

[17] R. Roth, H. Hergert, P. Papakonstantinou, T. Neff, and H. Feldmeier, Phys. Rev. C **72**, 034002 (2005).

[18] H. Feldmeier, T. Neff, R. Roth, and J. Schnack, Nucl. Phys. A **632**, 61 (1998).

[19] R. Roth, T. Neff, and H. Feldmeier, Prog. Part. Nucl. Phys. **65**, 50 (2010).

[20] A. Günther, R. Roth, H. Hergert, and S. Reinhardt, Phys. Rev. C **82**, 024319 (2010).

[21] A. Günther, P. Papakonstantinou, and R. Roth, J. Phys. G **41**, 115107 (2014).

[22] Mathworks, MATLAB, The Language of Technical Computing, 2014.

[23] S. G. Mallat, *A Wavelet Tour of Signal Processing* (Academic Press, New York, 1998).

[24] I. Pysmenetska, Doctoral thesis D17, Technische Universität Darmstadt, 2009.

[25] T. Guhr, A. Müller-Groeling, and H. A. Weidenmüller, Phys. Rep. **299**, 189 (1998).

[26] T. Ericson and T. Mayer-Kuckuk, Annu. Rev. Nucl. Part. Sci. **16**, 183 (1966).

[27] K. Eberhard and A. Richter, in *Proceedings of the International Conference on Statistical Properties of Nuclei*, edited by J. B. Garg (Plenum, New York, 1972), p. 139.